PAPER • **OPEN ACCESS**

Oscillatory behavior of *P* wave duration and *PR* interval in experimental congestive heart failure: a preliminary study

IOP Publishing Physiol. Meas. 39 (2018) 035010 (10pp) https://doi.org/10.1088/1361-6579/aaacab

Physiological Measurement

IPEM Institute of Physics and Engineering in Medicine

OPEN ACCESS

RECEIVED
19 July 2017

REVISED
29 January 2018

ACCEPTED FOR PUBLICATION
2 February 2018

PUBLISHED
29 March 2018

PAPER

Oscillatory behavior of *P* wave duration and *PR* interval in experimental congestive heart failure: a preliminary study

Gianfranco Piccirillo[1,2], Damiano Magrì[3], Gaetana D'Alessandro[1], Claudia Fiorucci[1], Federica Moscucci[1], Claudia Di Iorio[1], Fabiola Mastropietri[1], Ilaria Parrotta[1], Masahiro Ogawa[2,4], Shien-Fong Lin[2] and Peng-Sheng Chen[2]

[1] Dipartimento di Scienze Cardiovascolari, Respiratorie, Nefrologiche, Anestesiologiche e Geriatriche, Policlinico Umberto I, 'La Sapienza' University of Rome, Rome, Italy
[2] Division of Cardiology, Department of Medicine, Krannert Institute of Cardiology, Indiana University School of Medicine, Indianapolis, IN, United States of America
[3] Dipartimento di Medicina Clinica e Molecolare, S. Andrea Hospital, 'Sapienza' University of Rome, Rome, Italy
[4] Department of Cardiology, Fukuoka University School of Medicine, Fukuoka, Japan

E-mail: gianfranco.piccirillo@uniroma1.it

Keywords: chronic heart failure, *P* wave, autonomic nervous system, arrhythmias, vagal nerve activity (VNA), stellate ganglion nerve activity (SGNA), heart rate variability (HRV)

Abstract

Objective: The relationship between the autonomic nervous system (ANS) modulation of the sinus node and heart rate variability has been extensively investigated. The current study sought to evaluate, in an animal experimental model of pacing-induced tachycardia congestive heart failure (CHF), a possible ANS influence on the *P* wave duration and PR interval oscillations. *Approach*: Short-term (5 min) time and frequency domain analysis has been obtained in six dogs for the following electrocardiographic intervals: *P* wave duration (*P*), from the onset to peak of *P* wave (P_p), from the onset of *P* wave to the *q* onset (*PR*) and from the end of *P* wave to the onset of *q* wave (P_eR). Direct vagal nerve activity (VNA), stellate ganglion nerve activity (SGNA) and electrocardiogram (ECG) intervals have been evaluated contextually by implantation of three bipolar recording leads. *Main results*: At the baseline, multiple regression analysis pointed out that VNA was strongly positively associated with the standard deviation of *PP* and P_eR intervals (r^2:0.997, $p < 0.05$). The same variable was also positively associated with high-frequency (HF) of *P* expressed in normalized units, of P_p, and of P_eR (*b*: 0.001) (r^2: 0.993; $p < 0.05$). During CHF, most of the time and frequency domain variability significantly decreased from 20% to 50% in comparison to the baseline values ($p < 0.05$) and SGNA correlated inversely with the low frequency (LF) obtained from P_eR ($p < 0.05$) and *PR* ($p < 0.05$) (r^2:0.899, $p < 0.05$). LF components, expressed in absolute and normalized power, obtained from all studied intervals, were reduced significantly during CHF. Any difference between the *RR* and *PP* spectral components was observed. *Significance*: The data showed a significant relationship between ANS and atrial ECG variables, independent of the cycle duration. In particular, the oscillations were vagal mediated at the baseline, while sympathetic mediated during CHF. Whereas *P* wave variability might have a clinical utility in CHF management, it needs to be addressed in specific studies.

Introduction

It is well known that acute or chronic increase of left ventricular end-diastolic pressure, induced by several pathological conditions, could fatally induce a change in both atrial structure and function. Accordingly, in chronic heart failure (CHF) (Joung *et al* 2010a, 2010b) the electromechanical atrial remodeling, the sinus node dysfunction and supraventricular arrhythmias have been described. During healthy condition, the autonomic nervous system (ANS) modulates the sinus node activity, leading to the well-known oscillatory behavior of heart rate, due to the opposite and alternating vagal and sympathetic activity. Conversely, several cardiovascular

diseases are often associated with ANS imbalance with a sympathetic over-activity, which in turn is able to provoke a significant reduction of the heart rate variability (HRV) (Mortara *et al* 1994, Guzzetti *et al* 1995, Piccirillo *et al* 2006, 2009a). Thus, the oscillatory activity of the sinus node constantly and indirectly may provide useful insight into atrial and ventricular functions (Piccirillo *et al* 2016a, 2016b). Oscillatory activity originates in the sinus node and it spreads to the atria, the atrioventricular node and then to the ventricles. Although the *RR* interval variability is thought to be an exact surrogate of the *PP* interval variability, these two electrocardiographic intervals pertain to different cardiac chambers. Indeed, both atrial and ventricular damage could affect the supraventricular conduction system and hence the *PP* oscillations precede temporally those of the *RR* intervals (Horner *et al* 1996). The abovementioned extreme sensitivity of the supraventricular conduction systems to possible structural and functional heart changes raises interest in investigating possible earlier markers of ANS imbalance.

The previous studies on the HRV during CHF, focusing on the *RR* intervals, reported an *RR* variability reduction, expressed as time and frequency domain variables in short- and long-period electrocardiogram (ECG) recordings. In particular, in CHF the reduction of an RR spectral component, called low-frequency (LF) power, was related to the increase of left ventricular end diastolic pressure (Horner *et al* 1996), sinus dysfunction (Piccirillo *et al* 2009b), clinical progression of disease (Mortara *et al* 1994, Guzzetti *et al* 1995, Van de Borne *et al* 1997, Piccirillo *et al* 2004, 2006, Sanders *et al* 2004) and, moreover, the risk of sudden cardiac death (La Rovere *et al* 2003) and mortality (Guzzetti *et al* 2005) in both human and experimental models.

Obviously, the *RR* and *PP* power spectral analysis showed similar results and were then extensively studied, but we have few data on the intrinsic oscillations of the *P* wave and *PR* segment in CHF and in relation to autonomic control. Previous observations showed a reduction of *PQ–PP* and P_p–*PP* spectral coherence in CHF patients in comparison with normal subjects; these data could indicate atrial distress during an increase of left ventricular end-diastolic pressure and atrial enlargement.

The aim of this study was to evaluate the influence of ANS on the *P* wave and *PR* interval oscillations in CHF in order to understand if these variables could be used as a marker of autonomic influence, compared to the direct recording of stellate ganglia and vagal nerve activities (VNAs), on sinus and atrioventricular nodes.

Materials and methods

Surgical preparation and electrical recording

The data analyzed came from a previous study conducted in six female dogs (Ogawa *et al* 2007, Choi *et al* 2010, Han *et al* 2012). The surgical procedures and temporal relationship between cardiac arrhythmia and ANS activity are reported in detail elsewhere (Ogawa *et al* 2007, Choi *et al* 2010, Han *et al* 2012). Briefly, a pacing lead was implanted in the right ventricular apex and connected to an Itrel neurostimulator (Medtronic, Minneapolis, MN, USA) in a subcutaneous pocket. We then implanted a Data Sciences International (DSI) D70-EEE transmitter with three bipolar recording channels for simultaneous recording of the left stellate ganglion nerve activity (SGNA), VNA from the left thoracic vagal nerve located above the aortic arch, and subcutaneous ECG. After implantation, the Itrel stimulator was initially turned off for two weeks to allow the dogs to recover from surgery and to allow us to obtain the baseline recordings. The stimulator was then programmed to pace at 150 bpm for 3 d, at 200 bpm for 3 d, and then at 250 bpm for 3 weeks to induce CHF. The pacemaker was then turned off to allow an additional two weeks of ambulatory monitoring and recording during CHF. All CHF data were recorded within the first week. All animals underwent the same protocol with regard to intensity and duration of pacing. The animal experiments were approved by the Institutional Animal Care and Use Committee of the Cedars-Sinai Medical Center, Los Angeles, California.

Direct measurement of autonomic nervous activity

Data were recorded in real time at a sampling rate of 1000 samples s^{-1} per channel, then analyzed off-line. The software used has been described elsewhere (Ogawa *et al* 2007, Choi *et al* 2010, Han *et al* 2012). In brief, to analyze long-term trends in the large segmented data files effectively, a custom-designed program was developed using Labview™ (National Instruments, Austin, Texas, USA) software to automatically import, filter and analyze the DSI transmitter data for ANS activities and heart rates. The software determined the activation cycle length (*RR* intervals) automatically derived from the ECG (based on a Hilbert transform algorithm (Benitez *et al* 2001). Integrated data from the SGNA and VNA were high-pass (200 Hz) filtered and rectified over a fixed time segment to represent the total nerve activity. Because *RR* intervals shorter than 200 ms were usually due either to ectopic beats, artifacts or rhythm disturbances, they were removed and excluded from the analysis.

To assess ANS activity, we randomly selected six short-term recordings (5 min ECG) for each dog at the baseline and after pacing-induced CHF. Moreover, nerve activity data were also calculated over 24 h, namely in a total of 288 of 5 min epochs; finally, we calculated the means of these data and reported them as 24 h SGNA and VNA.

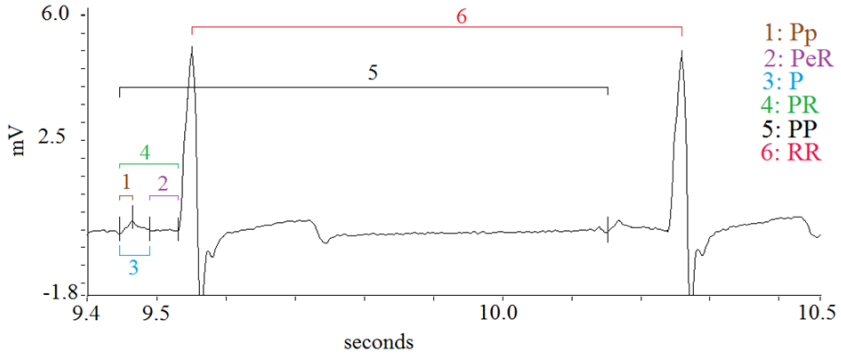

Figure 1. P_p (1), P_eR (2), PR (4), PP (5), RR (6) intervals and P (3) wave duration.

HRV power spectral analysis

We calculated the following intervals from 5 min epochs of ECG recordings: *RR*, *PP*, *P* wave (from onset to end of *P* wave), *PR* (from the onset of *P* wave to onset of *q* wave), and P_p (between the onset and the peak of *P* wave) and P_eR (from the end of *P* wave to the onset of *q* wave) intervals (figure 1).

We measured the mean, variance and standard deviation (SD) values for each interval. In particular, the value obtained for each variable was the mean of six-sample measurements before and after pacing-induced CHF, in the six dogs studied.

We used an autoregressive algorithm to compute the power spectral density from the different ECG variables (Task Force of the European Society of Cardiology and the North American Society of Pacing and Electrophysiology 1996). From a series of 5 min of consecutive beats, the autocorrelation function was applied to the complete *RR*, P_p, *PR*, *P*, P_eR, and *PP* series, and the Yule–Walker matrix (autocorrelation value matrix) was calculated with the Levinson–Darbin method; the matrix order was determined with an Anderson test and Akaike Information Criteria. The spectral decomposition method was then applied for the estimation of power and central frequency of each spectral component. Spectral power of each variable is expressed in milliseconds squared. The frequencies of the *RR*, P_p, *PR*, *P*, P_eR, and *PP* oscillations divided by the mean *RR*, P_p, *PR*, *P*, P_eR, and *PP* values, respectively expressed in milliseconds, were calculated in cycles per beat and converted to herz equivalents. We then determined the following power spectral variables in absolute power expressed in milliseconds squared of the *RR*, P_p, *PR*, *P*, P_eR, and *PP* intervals: total spectral power (TP) or root square of variance are expressed as SD; the high-frequency (HF) component (from 0.15–0.40 Hz); LF component (from 0.04–0.15 Hz) (Piccirillo *et al* 2004, 2009a, Magrì *et al* 2012).

Thereafter, the coherence function for the RR and the various repolarization intervals was estimated (Piccirillo *et al* 2009a, 2016a, 2016b, Baumert *et al* 2016). Coherence expresses the power fraction oscillating at a given frequency in either time series and is explained as a linear transformation of the other, thus indicating a linear association between the two signals. The coherence function $\gamma(f)$ was then computed according to the formula:

$$\text{Coherence}\,(f)\,\frac{|P_{xy}(f)|^2}{P_{xx}(f)P_{yy}(f)}$$

where f is frequency, $P_{xx}(f)$ is the spectrum of an obtained variable (*PR*, P_p, *P* or *RR*), $P_{yy}(f)$ are the other studied spectral variables (*PP*, *PR*, or P_eR), and $P_{xy}(f)$ is the cross-spectrum (*PR*–*PP*, P_p–*PP*, *P*–*PR*, *P*–P_eR, or *RR*–*PP*).

The coherence function provides a measure between zero and unity in the degree of linear interaction between the different studied interval oscillations as a function of their frequency. Mean coherences were measured by averaging $\gamma(f)$ over the frequency bands: from 0–0.50 Hz.

To detect the ECG intervals, we used a classic adaptive first derivative/threshold algorithm, explained elsewhere (Arzeno *et al* 2008). Also, to acquire, store and analyze the ECG data, we used our designed and produced software using Labview™ (National Instruments, Austin, Texas, USA). A cardiologist (GP) checked the different ECG wave and intervals, automatically marked by the software, and, when needed, manually corrected the mistakes. The premature beats and excessive noise were causes of possible mistakes in the interval measurement, so we have not considered in the analysis recordings with more than three premature beats.

At the baseline and after the pacing-induced CHF, the left ventricular ejection fraction, by echocardiographic study, and plasma levels of norepinephrine N-terminal and pro-B type natriuretic peptide (NT-proBNP) were evaluated.

Statistical analysis

Unless otherwise indicated, all data are expressed as mean ± SD. Data with skewed distribution are given as median and interquartile range (75th percentile—25th percentile).

Table 1. ECG variables at the baseline and during CHF.

Variables	Baseline $N = 6$	CHF $N = 6$	P values
RR mean, ms	768 ± 66	651 ± 97	NS
RR SD,	300 ± 44	160 ± 48	0.009
PP mean, ms	767 ± 67	651 ± 96	NS
PP SD,	305 ± 40	161 ± 47	0.006
P_p mean, ms	48 ± 17	49 ± 19	NS
P_p SD,	9 ± 3	7 ± 2	0.032
PR mean, ms	149 ± 30	143 ± 23	NS
PR SD,	7 ± 2	5 ± 2	0.020
P mean, ms	95 ± 26	91 ± 25	NS
P SD,	10 ± 3	8 ± 2	0.047
P_eR mean, ms	54 ± 9	53 ± 8	NS
P_eR SD,	9 ± 2	4 ± 2	0.000
PR–PP, coherence	0.275 ± 0.111	0.161 ± 0.028	0.048
P_p–*PP*, coherence	0.317 ± 0.075	0.223 ± 0.069	0.030
P–PR, coherence	0.564 ± 0.126	0.654 ± 0.111	NS
P–P_eR, coherence	0.666 ± 0.065	0.488 ± 0.167	0.014
RR–PP, coherence	0.970 ± 0.038	0.961 ± 0.030	NS
SGNA (μV/sample)	0.29 ± 0.20	0.43 ± 0.24	0.039
VNA (μV/sample)	0.11 ± 0.02	0.14 ± 0.06	NS
SGNA 24 h (μV/sample)	0.47 ± 0.09	0.62 ± 0.31	0.0001
VNA 24 h (μV/sample)	0.009 ± 0.003	0.026 ± 0.02	0.0001

Data are expressed as mean ± SD. SGNA: integrated left stellate ganglion nerve activity; VNA: integrated vagal nerve activity. NS: not significant.

In the present study, we analyzed six ECG registrations for the dogs at the baseline and after pacing-induced CHF. Therefore, we used the mean of six values for each variable for the statistical analysis at the baseline and after pacing-induced CHF. In conclusion, each variable was measured 36 (six dogs for six recordings) times before and after pacing-induced CHF.

The paired *t*-test was used to compare data for the normally distributed variables (including mean and SD of ECG variables, coherence functions, etc), whereas the Wilcoxon test was used to compare non-normally distributed variables (including variance and spectral components in absolute power of *RR*, P_p, *PR*, *P*, P_eR, and *PP* intervals and plasma levels of norepinephrine and NT-proBNP) at the baseline and after CHF. A stepwise multiple regression analysis was constructed to study possible associations between variables. In particular, we consider SGNA or VNA as a dependent variable and spectral and non-spectral (*RR*, P_p, *PR*, *P*, P_eR, and *PP*) studied data as independent variables at the baseline and after pacing-induced CHF.

Results

After pacing-induced CHF, in all six dogs, we obtained a significant reduction of ejection fraction ($p < 0.0001$) and a significant increase of norepinephrine ($p < 0.01$) and NT-proBNP levels in peripheral blood flow ($p < 0.05$) (Ogawa *et al* 2007). The voltage of the *P* wave was not significantly different between the baseline and CHF.

During the CHF period, the SDs of all variables (*RR*, *PP*, P_p, *P*, and P_eR) showed a significant reduction in comparison with the baseline period ($p < 0.05$) (table 1).

Similarly, the TP of each variable was lower during CHF. Finally, during CHF, *PR–PP*, P_p–*PP*, and *P*–P_eR spectral coherences were lower than at the baseline condition ($p < 0.05$ for all) (table 1).

In short-term study conditions, only the SGNA value was significantly higher during CHF ($p < 0.05$) (table 1). Conversely, both the 24 h SGNA ($p < 0.0001$) and 24 h VNA were significantly higher ($p < 0.0001$) during CHF (table 1).

LF, expressed in absolute power, was significantly lower during CHF in all studied variables (P_p, *P*, *PR* and P_eR) (figure 2).

LF, expressed in normalized units (NUs), confirmed the same behavior only for P_p and *PR* (figure 3).

Conversely, only HF absolute power of *P* was significantly lower during CHF in comparison with the baseline (baseline median: 42 ms^2, interquartile range: 46 ms^2 versus CHF median: 21 ms^2, interquartile range: 10 ms^2). We did not find any difference in the matrix order between the baseline and CHF period (baseline 17 ± 8 versus CHF: 20 ± 6, *p*: ns). We did not observe any difference between the *RR* and *PP* spectral components.

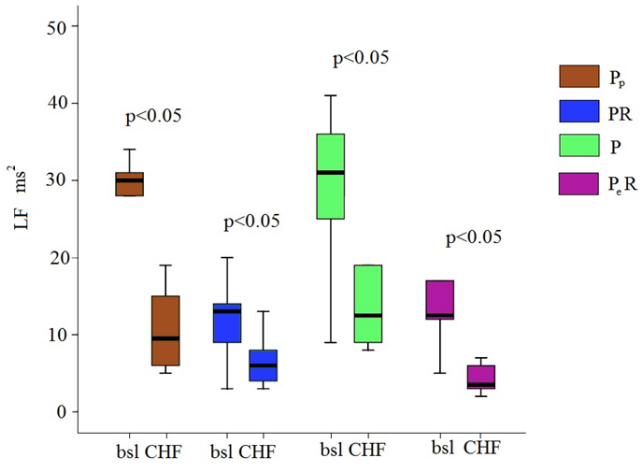

Figure 2. LF component of different tested variables at the baseline (bsl) and after pacing-induced tachycardia CHF. In the box plots, the central line represents the median distribution. Each box spans from the 25th to 75th percentile points, and error bars extend from the 10th to 90th percentile points.

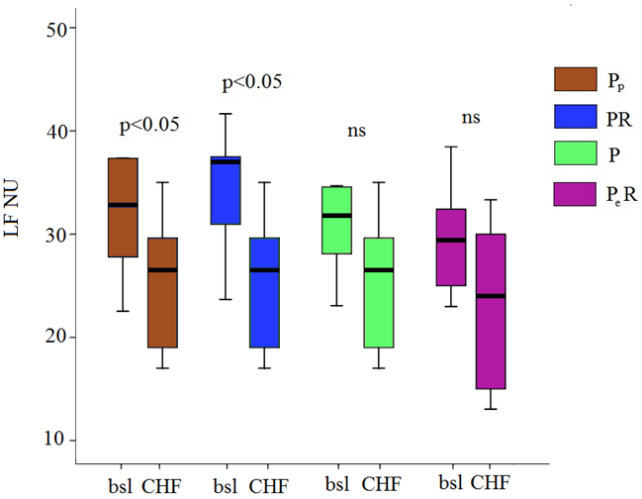

Figure 3. Comparisons of LF, expressed in NUs, at the baseline and after pacing-induced tachycardia CHF. In the box plots, the central line represents the median distribution. Each box spans from the 25th to 75th percentile points, and error bars extend from the 10th to 90th percentile points.

With regard to short-term time and frequency domain data, the stepwise multiple regression analysis showed a significant inverse relation at the baseline between SGNA and P_eR SDs (r: 0.937; b: $-$ 0.180, $p < 0.05$) and the HF of P (r: 0.912; b: $-$ 0.016, $p < 0.05$), expressed in NUs (figure 4).

In contrast, the VNA was positively associated with SD of PP (b: 0.002) and P_eR (b:0.000) intervals (r:0.9998, $p < 0.05$) (figure 5(A)). The same nerve variable was also positively associated with the HF of P expressed in NUs (b:0.002), of P_p (b:0.000), and of P_eR (b:0.001) (r:0.998; $p < 0.05$) (figure 5(B)).

Conversely, during CHF, the stepwise multiple regression analysis showed just a significant inverse relation between SGNA and the LF of P_eR, expressed in NUs, (r:0.948; b: $-$0.027, $p < 0.01$) (figure 6).

Discussion

The major and novel finding of the study was that pacing-induced tachycardia CHF produced a reduction of the temporal variability of the P wave duration and of P_p, P_eR, and PR intervals. In particular, all the short-term atrial ECG time-variables showed a reduction, expressed in SD, in CHF. Contextually, during CHF, a global reduction of LF power has been observed.

In fact, changes in the ANS modulation of the sinus node autonomic, together with a neuro-humoral and inflammatory activation, are common CHF features possibly related to an increased risk of atrial arrhythmias. A simultaneous increase in sympathetic and VNA has been described at the atrial level (Choi *et al* 2010, Han *et al* 2012), with the vagal activity increase being most likely a compensatory attempt to reduce the final sympathetic

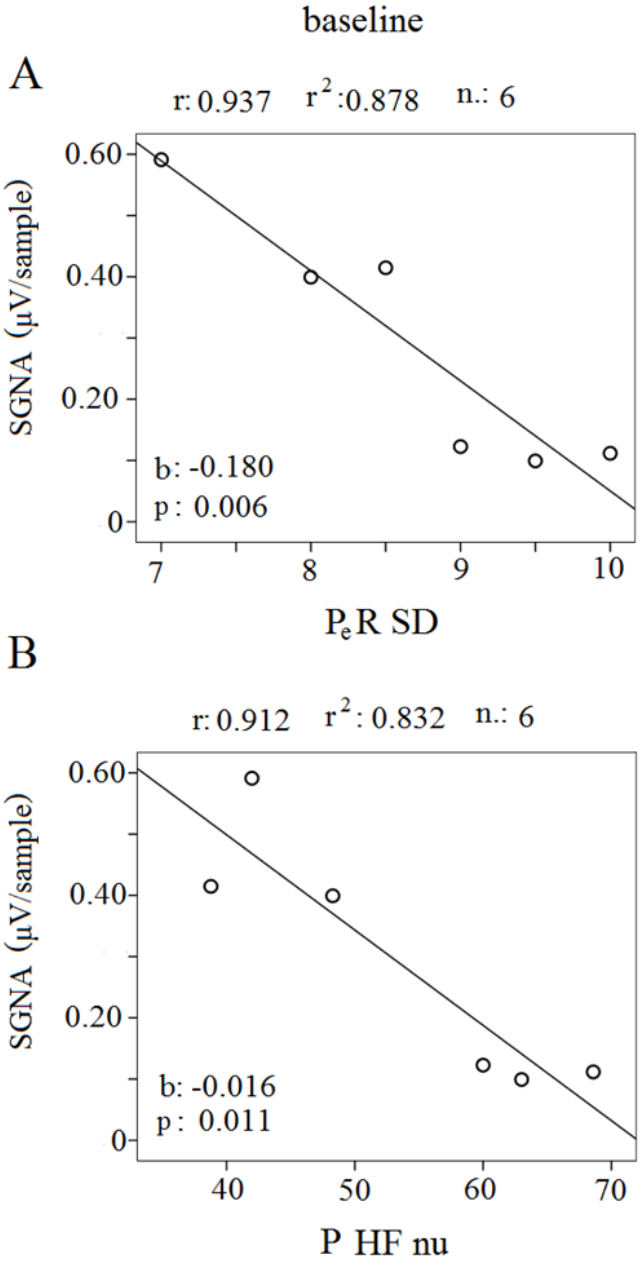

Figure 4. At the top panel (A), the multiple regression analysis between SGNA (dependent variable) and SD obtained from the P_eR interval at the baseline (significant independent variable). In (B), the same analysis between SGNA (dependent variable) and HF, expressed in NUs, obtained from the *P* wave duration at the baseline (significant independent variable).

hyperactivity. The abovementioned ANS imbalance leads to an increased temporal dispersion of refractory periods of the atrial myocytes, which in turn represents a trigger for atrial arrhythmias (i.e. atrial fibrillation). The observed reduction of variability of the atrial related ECG parameters during CHF, similar to those of the *RR* variability (Piccirillo *et al* 2009b), could be the direct consequence of this peculiar and proarrhythmic autonomic control (Piccirillo *et al* 2016a, 2016b). Interestingly, the reduced variability of these atrial variables was independent of the heart rate in this new experimental model (ECG recordings with similar heart rate analyzed) (Zaza and Lombardi 2001). In fact, in the pacing-induced CHF condition, we observed an equal level of VNA compared with the baseline even at the same heart rate. On the other hand, we found a higher VNA level on 24 h nerve recordings during CHF. Thus, although the higher levels of VNA could seem a paradox, it seems to be a compensatory mechanism to oppose the increase of SGNA (Choi *et al* 2010, Ogawa *et al* 2010, Han *et al* 2012). Further support to this VNA behavior, comes from the CHF-related upregulation of the muscarinic receptors (M2) reported in both human and animal models (DeMazumder *et al* 2015). Furthermore, this increase of vagal activity could be interpreted as an increase of vagal afferent activity related to the increase of end diastolic pressure and atrial distention in CHF.

Moreover, we observed that the VNA influenced prevalently the SD (time domain variables) of the P_eR and *PP* intervals and the HF (frequency domain variables) of the *P* wave duration at the baseline. Conversely, the

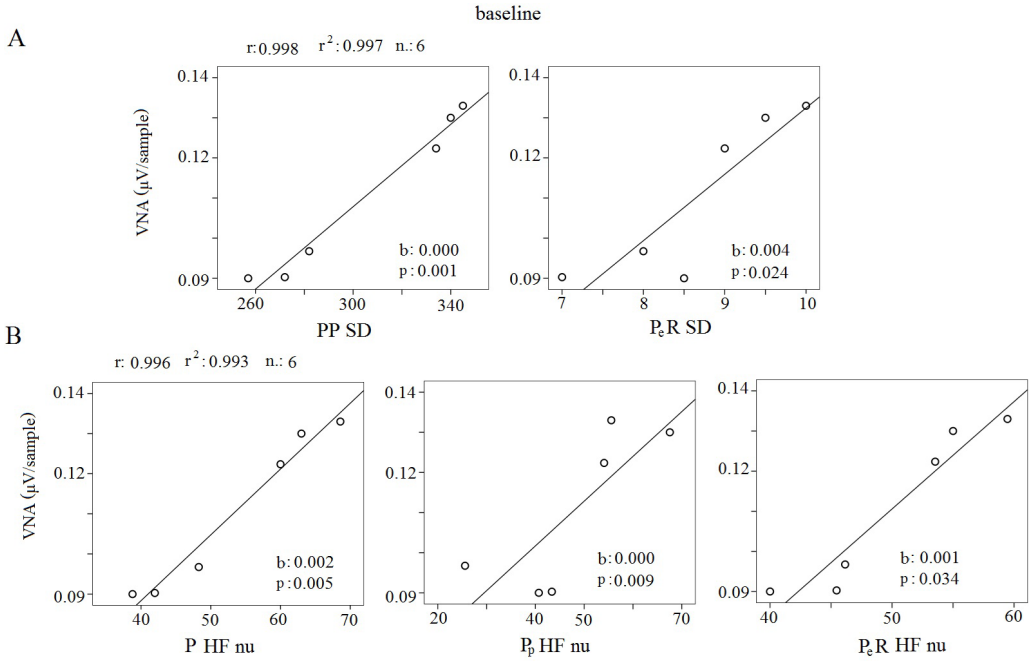

Figure 5. At the top panel (A) the multiple regression analysis between VNA (dependent variable) and *PP* intervals and SD obtained from the P_eR at the baseline (significant independent variables). In (B), the same analysis between VNA (dependent variable) and the HF, expressed in NUs, obtained from the *P* wave duration, P_p and P_eR intervals at the baseline (significant independent variables).

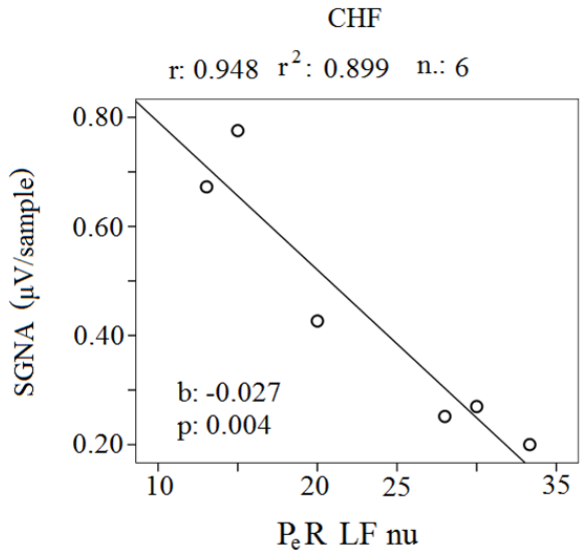

Figure 6. Multiple regression analysis between SGNA (dependent variable) and the LF, expressed in NUs, obtained from the P_eR intervals (significant independent variable) after pacing-induced tachycardia CHF.

SGNA had no influence on any atrial time domain variables. This finding is not unexpected, because the HRV expressed as SD in short-term ECG recordings is a marker of vagal activity (Task Force of the European Society of Cardiology and the North American Society of Pacing and Electrophysiology 1996) and, hence, the positive relation between VNA and the *PP* interval SD confirms that this parameter could be considered a noninvasive marker of vagal atrial activity under healthy condition. In fact, undiscussed specific papers in this field, albeit dated, reported that the vagal pharmacological suppression induces a dramatic reduction of the short period of SD of *RR* and for this reason, all spectral components (Pomeranz *et al* 1985, Koh *et al* 1994, Després *et al* 2002, Laude *et al* 2008). Finally, this reduction was found to be abolished in the absence of VNA (Epstein *et al* 1990). In addition, our data suggest that these atria variables are probably more reliable than RR variability for sinus vagal activity (i.e. stepwise multivariable analysis did not show a significant relation between *RR* SD and the VNA). Indeed, atria, sinus node and atrioventricular node are extensively innervated by parasympathetic nerves. Thus, we could consider that particularly the P_eR interval represents the best noninvasive surrogate of the electrical conduction between the atrioventricular node and the His bundle. On the other hand, the atrial spectral markers,

that is the HF of P_p and P, could express the effect of vagal influence on the right and left atria. In fact, the first part of the P wave, since the P peak is probably linked to the electrical depolarization of the right atrium (Puech *et al* 1974), whereas the total P wave duration is mainly influenced by the left atria. (Chirife *et al* 1975). In conclusion, these spectral variables were markers of vagal effect on both atria in normal condition (figure 5).

In power spectral and time domain atrial variables related to the SGNA, the influence seems to be partially coincident in baseline and CHF conditions. In fact, we found an inverse relation between SGNA and P_eR vagal-derived markers in both these experimental conditions. In particular, we found that SD and HF of P_eR are characterized by an inverse relationship, expressed in NUs. This datum could indicate that the sympathetic activity, recorded in the left stellate ganglion, induced a reduction of vagal activity in the atrioventricular node and in His bundle. Naturally, a large and historical pathophysiological literature reported that left side sympatho-vagal innervations, as in our study, had a prevalent influence on atrioventricular node function (Cohn *et al* 1913, Cinca *et al* 1985, Inoue *et al* 1987, Waninger *et al* 1999).

The inverse relationship between the left SGNA and VNA seemed to have only one possible and easy explanation: sympathetic activation was able to reduce the vagal activity in atrioventricular node and in His bundle in normal and CHF condition, inducing the well-known phenomenon called sympathetic-parasympathetic interaction in the A–V conduction system (Salata *et al* 1986, Levy *et al* 1988, Brack *et al* 2004, White *et al* 2014).

Although the physiological meaning of LF still remains controversial (Parati *et al* 1995, Sleight *et al* 1995, Task Force of the European Society of Cardiology and the North American Society of Pacing and Electrophysiology 1996, Moak *et al* 2007, Piccirillo *et al* 2009a), the Mayer waves, that cause these oscillations (about 0.10 Hz), are reduced in the CHF for the P_eR and PR segments in the same way as RR variability (van de Borne *et al* 1997, Piccirillo *et al* 2006). Moreover, both in human and in experimental CHF models, the LF reduction is related to severity of the disease and it is a marker of CHF-related mortality (Mortara *et al* 1994, van de Borne *et al* 1997, La Rovere *et al* 2003, Guzzetti *et al* 2005, Piccirillo *et al* 2009b). Thus, the LF reduction of atrial variables could be considered a noninvasive and inexpensive marker of the degree of dysfunction of the atrial and ventricular myocardium.

In conclusion, the atrial ECG-derived intervals showed oscillations similar to those of the RR interval and, in normal conditions, they seem to be controlled primarily by VNA. In contrast, during experimental CHF, the atrial ECG-derived intervals collapse dramatically, with these reductions related to increased sympathetic nerve activity. Thus, different atrial structures seemed to have different oscillatory behavior according to the autonomic control and the presence of CHF. The P wave duration and PR interval oscillation evaluation might be a stimulating idea for future research on paroxysmal supraventricular arrhythmias. Moreover, given that the ECG yields a simple and transmissible signal, this easy approach could be developed as a remote medical technology, thereby saving time and economic resources.

Study limitation

The most important study limitation was the small number of studied animals. However, it should be emphasized that we checked every point automatically found by the software for a total of about 150 000 points (five points for each beat). Analyzable recordings should be of good quality, avoiding confounding noise (resulting from environmental conditions, i.e. dog movements). Thus, we analyzed the study variables in 36 5 min ECG recordings at the baseline and after pacing-induced CHF (six baselines and six CHFs for each of the six cases). The abovementioned vast amount of work, which took nearly two years, led us to obtain measurements with a high level of accuracy.

Another possible limitation was that the HRV, SGNA and VNA were markers of ANS modulation as mean in 5 min rather than a marker of a moment-to-moment or instantaneous nerve activity. Because the HRV needed a stationary period (see figure 3), we also possibly choose a stationary period of nerve activity, and therefore the HRV, SGNA and VNA were numerically expressed as mean of 5 min.

The last technical limitation of direct nerve recording was undoubtedly that the adopted approach did not permit us to discriminate the afferent from efferent nerve activity. Therefore, we need to consider the possibility to have a pure efferent cardiovascular signal.

Conflict of interest

The authors declare no financial or industrial interests regarding this study.

ORCID iDs

Gianfranco Piccirillo https://orcid.org/0000-0002-6067-9962

References

Arzeno N M, Deng Z D and Poon C S 2008 Analysis of first-derivative based QRS detection algorithms *IEEE Trans. Biomed. Eng.* **55** 478–84

Baumert M, Porta A, Vos M A, Malik M, Couderc J P, Laguna P, Piccirillo G, Smith G L, Tereshchenko L G and Volders P G 2016 QT interval variability in body surface ECG: measurement, physiological basis, and clinical value: position statement and consensus guidance endorsed by the European Heart Rhythm Association jointly with the ESC Working Group on Cardiac Cellular Electrophysiology *Europace* **18** 925–44

Benitez D, Gaydecki P A, Zaidi A and Fitzpatrick A P 2001 The use of the Hilbert transform in ECG signal analysis *Comput. Biol. Med.* **31** 399–406

Brack K E, Coote J H and Ng G A 2004 Interaction between direct sympathetic and vagus nerve stimulation on heart rate in the isolated rabbit heart *Exp. Physiol.* **89** 128–39

Chirife R, Feitosa G S and Frankl W S 1975 Electrocardiographic detection of left atrial enlargement. Correlation of *P* wave with left atrial dimension by echocardiography *Br. Heart J.* **37** 1281–5

Choi E K *et al* 2010 Intrinsic cardiac nerve activity and paroxysmal atrial tachyarrhythmia in ambulatory dogs *Circulation* **121** 2615–23

Cinca J, Evangelista A, Montoyo J, Barutell C, Figueras J, Valle V, Rius J and Soler-Soler J 1985 Electrophysiologic effects of unilateral right and left stellate ganglion block on the human heart *Am. Heart J.* **109** 46–54

Cohn A E and Lewis T 1913 The predominant influence of the left vagus nerve upon conduction between the auricles and ventricles in the dog *J. Exp. Med.* **18** 739–47

DeMazumder D, Kass D A, O'Rourke B and Tomaselli G F 2015 Cardiac resynchronization therapy restores sympathovagal balance in the failing heart by differential remodeling of cholinergic signaling *Circ. Res.* **116** 1691–9

Després G, Veissier I and Boissy A 2002 Effect of autonomic blockers on heart period variability in calves: evaluation of the sympathovagal balance *Physiol. Res.* **51** 347–53

Epstein A E, Hirschowitz B I, Kirklin J K, Kirk K A, Kay G N and Plumb V J 1990 Evidence for a central site of action to explain the negative chronotropic effect of atropine: studies on the human transplanted heart *J. Am. Coll. Cardiol.* **15** 1610–7

Guzzetti S, Cogliati C, Turiel M, Crema C, Lombardi F and Malliani A 1995 Sympathetic predominance followed by functional denervation in the progression of chronic heart failure *Eur. Heart J.* **16** 1100–7

Guzzetti S, La Rovere M T, Pinna G D, Maestri R, Borroni E, Porta A, Mortara A and Malliani A 2005 Different spectral components of 24 h heart rate variability are related to different modes of death in chronic heart failure *Eur. Heart J.* **26** 357–62

Han S *et al* 2012 Electroanatomic remodeling of the left stellate ganglion after myocardial infarction *J. Am. Coll. Cardiol.* **59** 954–61

Horner S M, Murphy C F, Coen B, Dick D J, Harrison F G, Vespalcova Z and Lab M J 1996 Contribution to heart rate variability by mechanoelectric feedback. Stretch of the sinoatrial node reduces heart rate variability *Circulation* **94** 1762–7

Inoue H and Zipes D P 1987 Changes in atrial and ventricular refractoriness and in atrioventricular nodal conduction produced by combinations of vagal and sympathetic stimulation that result in a constant spontaneous sinus cycle length *Circ. Res.* **60** 942–51

Joung B *et al* 2010a Tachybradycardia in the isolated canine right atrium induced by chronic sympathetic stimulation and pacemaker current inhibition *Am. J. Physiol. Heart Circ. Physiol.* **299** H634–42

Joung B *et al* 2010b Mechanisms of sinoatrial node dysfunction in a canine model of pacing-induced atrial fibrillation *Heart Rhythm* **7** 88–95

Koh J, Brown T E, Beightol L A, Ha C Y and Eckberg D L 1994 Human autonomic rhythms: vagal cardiac mechanisms in tetraplegic subjects *J. Physiol.* **474** 483–95

La Rovere M T *et al* 2003 Short-term heart rate variability strongly predicts sudden cardiac death in chronic heart failure patients *Circulation* **107** 565–70

Laude D, Baudrie V and Elghozi J L 2008 Effects of atropine on the time and frequency domain estimates of blood pressure and heart rate variability in mice *Clin. Exp. Pharmacol. Physiol.* **35** 454–7

Levy M N 1988 Sympathetic-vagal interactions in the sinus and atrioventricular nodes *Prog. Clin. Biol. Res.* **275** 187–97

Magrì D *et al* 2012 Increased temporal dispersion of myocardial repolarization in myotonic dystrophy type 1: beyond the cardiac conduction system *Int. J. Cardiol.* **156** 259–64

Moak J P, Goldstein D S, Eldadah B A, Saleem A, Holmes C, Pechnik S and Sharabi Y 2007 Supine low-frequency power of heart rate variability reflects baroreflex function, not cardiac sympathetic innervation *Heart Rhythm* **4** 1523–9

Mortara A, La Rovere M T, Signorini M G, Pantaleo P, Pinna G, Martinelli L, Ceconi C, Cerutti S and Tavazzi L 1994 Can power spectral analysis of heart rate variability identify a high risk subgroup of congestive heart failure patients with excessive sympathetic activation? A pilot study before and after heart transplantation *Br. Heart J.* **71** 422–30

Ogawa M *et al* 2007 Left stellate ganglion and vagal nerve activity and cardiac arrhythmias in ambulatory dogs with pacing-induced congestive heart failure *J. Am. Coll. Cardiol.* **50** 335–43

Parati G, Saul J P, Di Rienzo M and Mancia G 1995 Spectral analysis of blood pressure and heart rate variability in evaluating cardiovascular regulation. A critical appraisal *Hypertension* **25** 1276–86

Piccirillo G *et al* 2006 Influence of cardiac-resynchronization therapy on heart rate and blood pressure variability: 1-year follow-up *Eur. J. Heart Failure* **8** 716–22

Piccirillo G *et al* 2009a Autonomic nervous system activity measured directly and QT interval variability in normal and pacing-induced tachycardia heart failure dogs *J. Am. Coll. Cardiol.* **54** 840–50

Piccirillo G *et al* 2009b Power spectral analysis of heart rate variability and autonomic nervous system activity measured directly in healthy dogs and dogs with tachycardia-induced heart failure *Heart Rhythm* **6** 546–52

Piccirillo G *et al* 2016a *P* wave analysis and left ventricular systolic function in chronic heart failure. Possible insights form the *P* wave—*PP* interval spectral coherence *Minerva Cardioangiol.* **64** 525–33

Piccirillo G *et al* 2016b Time- and frequency-domain analysis of beat to beat *P*-wave duration, *PR* interval and *RR* interval can predict asystole as form of syncope during head-up tilt *Physiol. Meas.* **37** 1910–24

Piccirillo G, Magrì D, Naso C, di Carlo S, Moisé A, De Laurentis T, Torrini A, Matera S and Nocco M 2004 Factors influencing heart rate variability power spectral analysis during controlled breathing in patients with chronic heart failure or hypertension and in healthy normotensive subjects *Clin. Sci.* **107** 183–90

Pomeranz B *et al* 1985 Assessment of autonomic function in humans by heart rate spectral analysis *Am. J. Physiol.* **248** H151–3

Puech P 1974 The *P* wave: correlation of surface and intra-atrial electrograms *Cardiovasc. Clin.* **6** 43–68

Salata J J, Gill R M, Gilmour R F Jr and Zipes D P 1986 Effects of sympathetic tone on vagally induced phasic changes in heart rate and atrioventricular node conduction in the anesthetized dog *Circ. Res.* **58** 584–94

Sanders P, Kistler P M, Morton J B, Spence S J and Kalman J M 2004 Remodeling of sinus node function in patients with congestive heart failure: reduction in sinus node reserve *Circulation* **110** 897–903

Sleight P, La Rovere M T, Mortara A, Pinna G, Maestri R, Leuzzi S, Bianchini B, Tavazzi L and Bernardi L 1995 Physiology and pathophysiology of heart rate and blood pressure variability in humans: is power spectral analysis largely an index of baroreflex gain? *Clin. Sci.* **88** 103–9

van de Borne P, Montano N, Pagani M, Oren R and Somers V K 1997 Absence of low-frequency variability of sympathetic nerve activity in severe heart failure *Circulation* **95** 1449–54

Waninger M S, Bourland J D, Geddes L A and Schoenlein W E 1999 Characterization of atrioventricular nodal response to electrical left vagal stimulation *Ann. Biomed. Eng.* **27** 758–62

White D W and Raven P B 2014 Autonomic neural control of heart rate during dynamic exercise: revisited *J. Physiol.* **592** 2491–500

Zaza A and Lombardi F 2001 Autonomic indexes based on the analysis of heart rate variability: a view from the sinus node *Cardiovasc. Res.* **50** 434–42

(Task Force of the European Society of Cardiology and the North American Society of Pacing and Electrophysiology) 1996 Heart rate variability: standards of measurement, physiological interpretation and clinical use *Circulation* **93** 1043–65